



## Regional characteristics of atmospheric $\delta^{34}\text{S}\text{-SO}_4^{2-}$ over three parts of Asia monitored by quartz wool-based passive samplers



Xiao Wang<sup>a,b,g</sup>, Jun Li<sup>a,b,c,\*</sup>, Rong Sun<sup>a,b,g</sup>, Hongxing Jiang<sup>a,b,g</sup>, Zheng Zong<sup>d</sup>, Chongguo Tian<sup>d</sup>, Luhua Xie<sup>e</sup>, Qilu Li<sup>f</sup>, Wanglu Jia<sup>a</sup>, Ping'an Peng<sup>a,b,c</sup>, Gan Zhang<sup>a,b,c</sup>

<sup>a</sup> State Key Laboratory of Organic Geochemistry and Guangdong province Key Laboratory of Environmental Protection and Resources Utilization, Guangzhou Institute of Geochemistry, Chinese Academy of Sciences, Guangzhou 510640, China

<sup>b</sup> CAS Center for Excellence in Deep Earth Science, Guangzhou 510640, China

<sup>c</sup> Guangdong-Hong Kong-Macao Joint Laboratory for Environmental Pollution and Control, Guangzhou Institute of Geochemistry, Chinese Academy of Science, Guangzhou 510640, China

<sup>d</sup> Key Laboratory of Coastal Environmental Processes and Ecological Remediation, Yantai Institute of Coastal Zone Research, Chinese Academy of Sciences, Yantai 264003, China

<sup>e</sup> Key Laboratory of Ocean and Marginal Sea Geology, Guangzhou Institute of Geochemistry, Chinese Academy of Sciences, Guangzhou 510640, China

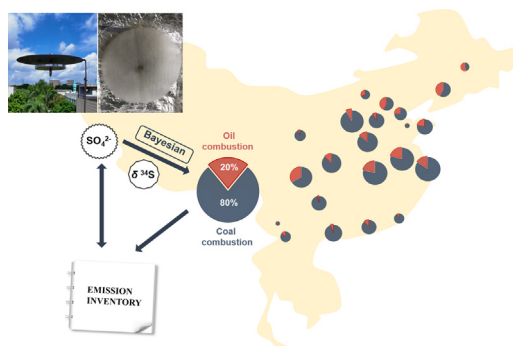
<sup>f</sup> School of Environment, Henan Normal University, Key Laboratory for Yellow River and Huai River Water Environment and Pollution Control, Ministry of Education, Henan Key Laboratory for Environmental Pollution Control, Xinxiang 453007, China

<sup>g</sup> University of Chinese Academy of Sciences, Beijing 100049, China

### HIGHLIGHTS

- A new method of PAS-QW was developed to monitor aerosol  $\delta^{34}\text{S}\text{-SO}_4^{2-}$ .
- The spatial heterogeneity of  $\text{SO}_4^{2-}$  content and  $\delta^{34}\text{S}$  was obvious in study areas.
- Coal and oil combustion are major sources of  $\text{SO}_2$ , but with difference between regions.

### GRAPHICAL ABSTRACT



### ARTICLE INFO

#### Article history:

Received 20 October 2020

Received in revised form 22 February 2021

Accepted 23 February 2021

Available online 5 March 2021

Editor: Xinbin Feng

#### Keywords:

China  
Indochina peninsula  
Pakistan  
Passive air sampler

### ABSTRACT

A new method is presented for measuring atmospheric contents and  $\delta^{34}\text{S}\text{-SO}_4^{2-}$  in airborne particulate matter using quartz wool disk passive air samplers (Pas-QW). The ability of Pas-QW samplers to provide time-integrated measurements of atmospheric  $\text{SO}_4^{2-}$  was confirmed in a field calibration study. The average sampling rate of  $\text{SO}_4^{2-}$  measured was  $2.3 \pm 0.3 \text{ m}^3/\text{day}$ , and this was not greatly affected by changes in meteorological parameters. The results of simultaneous sampling campaign showed that the average  $\text{SO}_4^{2-}$  contents in Pakistan and the Indochina Peninsula (ICP) were relatively lower than that of China. The spatial distribution of  $\text{SO}_4^{2-}$  concentrations was largely attributed to the development of the regional economies. The range of  $\delta^{34}\text{S}$  values observed in Pakistan ( $4.3 \pm 1.4\text{‰}$ ) and the ICP ( $4.5 \pm 1.2\text{‰}$ ) were relatively small, while a large range of  $\delta^{34}\text{S}$  values was observed in China ( $3.9 \pm 2.5\text{‰}$ ). The regional distribution of sulfur isotope compositions was significantly affected by coal combustion. A source analysis based on a Bayesian mixing model showed that  $80.4 \pm 13.1\%$  and  $19.6 \pm 13.1\%$  of artificial sulfur dioxide ( $\text{SO}_2$ ) sources in China could be attributed to coal combustion and oil combustion, respectively. The two sources differed greatly between regions, and the contribution of oil combustion in cities was higher than

\* Corresponding author at: State Key Laboratory of Organic Geochemistry and Guangdong Province Key Laboratory of Environmental Protection and Resources Utilization, Guangzhou Institute of Geochemistry, Chinese Academy of Sciences, Guangzhou 510640, China.

E-mail address: [junli@gig.ac.cn](mailto:junli@gig.ac.cn) (J. Li).

## 1. Introduction

Sulfate ( $\text{SO}_4^{2-}$ ) acting as cloud condensation nuclei is a substantial component of atmospheric aerosols (Matsumoto et al., 1997). Such  $\text{SO}_4^{2-}$  aerosols affect the surface temperature of the Earth (Charlson et al., 1992), acid rain formation (Charlson et al., 1992; Zhang et al., 1995), and human health (Pope and Dockery, 2006), and play a key role in environmental chemistry and climate change (Abbatt et al., 2006). Therefore, knowing the sources of aerosol  $\text{SO}_4^{2-}$  and its transport and transformation in the atmosphere forms a necessary basis for improving air quality (Chen et al., 2013). The main primary sources of atmospheric  $\text{SO}_4^{2-}$  are sea salt, dust, and fly ash (Sinha et al., 2008; Tostevin et al., 2014). Secondary sources arise from gas- or aqueous-phase oxidation processes of anthropogenic sulfur dioxide ( $\text{SO}_2$ ) emitted from fossil fuel combustion, industrial processes and biomass burning activities, and from oxidation products of natural sulfur-containing compounds, such as dimethylsulfide (DMS) (Amrani et al., 2013) and hydrogen sulfide ( $\text{H}_2\text{S}$ ) (Sinha et al., 2008).

$\text{SO}_4^{2-}$  emitted from different sources has different  $\text{SO}_4^{2-}$  isotopic signals ( $\delta^{34}\text{S}$ ). Numerous studies have been carried out in Europe (Sinha et al., 2008), the Arctic (Kunasek et al., 2010), America (Calhoun et al., 1991), and China (Han et al., 2016; Mukai et al., 2001) using  $\delta^{34}\text{S}$  to trace  $\text{SO}_4^{2-}$  source in aerosol particles and precipitation. The  $\delta^{34}\text{S}$  values of different anthropogenic and natural sources usually vary widely (Fig. S1 in the Supporting Information). The range of  $\delta^{34}\text{S}$  values from natural sources is from  $-10$  to  $+20\%$ , of which the  $\delta^{34}\text{S}$  of sea salt  $\text{SO}_4^{2-}$ , DMS, and biogenic sulfur released from soils and wetlands is  $+20.1\%$  (Tostevin et al., 2014),  $+18$  to  $+21\%$  (Amrani et al., 2013), and  $-10$  to  $-2\%$  (Lei et al., 1997), respectively. The range of  $\delta^{34}\text{S}$  value of anthropogenic sulfate is  $-2$  to  $+18\%$  (Han et al., 2016; Norman et al., 1999). The anthropogenic input of sulfur compounds to the atmosphere through deposition is a major source of atmospheric  $\text{SO}_4^{2-}$ , which could be elucidated from the sulfur isotopic signature (Calhoun et al., 1991; Han et al., 2016; Mukai et al., 2001). Analysis of the stable sulfur isotopes within atmospheric-derived  $\text{SO}_4^{2-}$  ( $\delta^{34}\text{S}$ - $\text{SO}_4^{2-}$ ) can provide a powerful tool to apportion  $\text{SO}_2$  sources, because atmospheric  $\text{SO}_4^{2-}$  is primarily formed by the oxidation of  $\text{SO}_2$  in the Northern Hemisphere. The main way to reduce the adverse effects of the sulfate on human health and atmospheric environment is to control the emission of the precursor  $\text{SO}_2$  (Li et al., 2017b; Ohizumi et al., 2016; Sinha et al., 2008). Combining isotope techniques with stable isotope models permits good estimation of the contribution of different sources in a mixture. Recently, the Bayesian model was adopted to apportion major sources of atmospheric nitrogen oxides based on  $\delta^{15}\text{N}$ - $\text{NO}_3^-$  values (Zong et al., 2017), this provides a good example for the quantification of  $\text{SO}_2$  sources. However, further exploration is needed of methods to incorporate the possible fractionation effect into a Bayesian model.

Passive samplers have been used to monitor organic and inorganic pollutants in various indoor and outdoor environments (Demirel et al., 2014; Gaga et al., 2019; Jiang et al., 2018). Compared with active samplers, they are easy to use, require less maintenance and infrastructure/electricity to operate, and have a small size, making them ideally suited to spatial investigations of air pollutants (Eng et al., 2014; Jiang et al., 2018). The prototype passive dry deposition (Pas-DD) collector is a kind of versatile and cost-effective passive sampler for studying organic chemicals over large regions (Eng et al., 2014; Gaga et al., 2019). Harner et al. (Gaga et al., 2019) recently developed a sampling method for measuring trace metals collected by Pas-DD collectors, and different

metals were shown with different equivalent air sampling rates. This provides a proof concept and methodology for the use of Pas-DD as a promising tool for monitoring studies of both organic and inorganic pollutants in air. Quartz fiber is commonly used as a material for collecting atmospheric particulates (Jiang et al., 2018; Norman et al., 2006; Zong et al., 2017). As one kind of quartz fiber with a larger specific surface area, the quartz wool disk passive air sampler (Pas-QW) may provide a better measurement of organic and inorganic particulate matter (PM) compared with the traditional polyurethane foam disk (PUF) used inside Pas-DD. It can eliminate the matrix interference of PUF and have a good contrast with other studies.

Combined with passive sampling technologies, it is possible to conduct top-down observations based on source-diagnostic stable sulfur isotopes over large regions. In this study, our objectives were to (i) develop sampling methods for measuring  $\text{SO}_4^{2-}$  collected by a Pas-QW collector, (ii) conduct a campaign of passive sampling in three regions of Asia to assess the spatial distribution of atmospheric  $\text{SO}_4^{2-}$  contents and  $\delta^{34}\text{S}$  values, and (iii) combine the Bayesian model to quantitatively apportion the respective contribution of major artificial sources and compare them with recent  $\text{SO}_2$  emission inventories in China.

## 2. Materials and methods

### 2.1. Calibration exercise for sulfate

A schematic of the Pas-QW used in this study is shown in Fig. S2. Similar to the Pas-DD, the sampler consists of a stainless-steel plate cover and a small stainless-steel pan. A quartz wool disk (14.0 cm diameter, 1.35 cm thickness, 367  $\text{cm}^2$  surface area, 1.0 g mass, 207  $\text{cm}^3$  volume, and 0.005  $\text{g}/\text{cm}^3$  density) was placed inside the pan and covered with a stainless-steel mesh ( $1 \times 1$  cm). Two batches of Pas-QW from different time periods and regions were arranged in the field deployments for better contrast. The first batch of 12 passive samplers was set up and deployed from August to October 2016 over a 70-day period in Guangzhou (GZ). The second batch of 12 passive samplers was set up and deployed from January to April 2019 over a 77-day period in Yantai (YT). Neither of the sampling sites had any obvious point emission sources nearby. Over the period, active air sampling (AAS) was conducted continuously alongside passive sampling throughout the calibration exercise. The AAS was set at an identical height for deployment of the passive sampler and total suspended particle samples were collected on prebaked quartz fiber filters ( $18.0 \times 10.5$   $\text{cm}^2$ ). The samples were collected for a 2–7-day duration at a stable flow rate of 300 L/min. Detail information on the calibration exercise is provided in Text S1. The active sampling time did not always exactly match the retrieval time of the Pas-QW samplers due to unavoidable factors including power supply interruption, heavy rainfall, and typhoons (Tables S1 and S2). In this case, the average concentrations of  $\text{SO}_4^{2-}$  derived from active sampling during the corresponding deployment time of the Pas-QW were used as the reference air concentrations during the calibration exercise.

The sampling rate ( $R'$ ) of pollutants can be expressed as

$$R' = \frac{m_{PAS}}{C_{air}t} \quad (1)$$

where  $R'$  is the sampling rate for air ( $R'$ ,  $\text{m}^3/\text{day}$ ),  $m_{PAS}$  is the accumulated mass of the target compound collected by each quartz wool disk during the exposure period ( $m_{PAS}$ ,  $\mu\text{g}$ ),  $C_{air}$  is the air concentration of

$\text{SO}_4^{2-}$  determined by AAS ( $C_{\text{air}}, \mu\text{g}/\text{m}^3$ ), and  $t$  is the sampling time (days). The equivalent air volumes ( $V_{\text{eq}}, \text{m}^3$ ) sampled by Pas-QWs were determined on the basis of the reported ambient air concentrations of the  $\text{SO}_4^{2-}$  and their accumulated mass on the passive samplers.

$$V_{\text{eq}} = \frac{m_{\text{PAS}}}{C_{\text{air}}} \quad (2)$$

$R'$  was determined from the slope of the line of best fit between  $V_{\text{eq}}$  and time.

## 2.2. Field sample collection

22 air-monitoring stations were selected as sampling sites in China from March to June in 2017, and 2 air-monitoring stations and 5 air-monitoring stations were selected in Pakistan and the ICP from March to June in 2016. These included 21 urban sites, 6 rural or suburban sites and 2 background sites. Details of each sampling site and basic related parameters are provided in Tables S3 and S4. Samplers were assembled at the deployment sites to avoid contamination during transportation. After deployment, the quartz wool disks were retrieved, resealed, and returned to Guangzhou, where they were stored in a fridge at  $-20^\circ\text{C}$  before analysis.

## 2.3. Chemical and isotopic measurements

The quartz wool disk samples were soaked in 40 mL of Milli-Q water for 30 min then subjected to ultrasonification. The samples were kept in the water for 12 h to thoroughly extract the water-soluble ions (Norman et al., 2006). A 5-mL sample was withdrawn from the filtered solution for ion concentration analysis. The remaining solution was acidified to  $\text{pH} < 2$  by addition of HCl solution, then the dissolved  $\text{SO}_4^{2-}$  in the solution was trapped as barite ( $\text{BaSO}_4$ ) by addition of droplets of supersaturated  $\text{BaCl}_2$  solution. The  $\text{BaSO}_4$  precipitates were separated by centrifugation, rinsed with Milli-Q water several times to remove chloride ion, and precipitates were dried in an oven at  $50^\circ\text{C}$  for 24 h. The blank samples were analyzed using the same method (Text S2).

Concentrations of water-soluble ions were measured via ion chromatography (Dionex ICS3000; Dionex Ltd., Sunnyvale, CA, USA) based on the reported analysis method (Wang et al., 2019). The relative standard deviation of repetitive measurements was less than 5% for each ion. The detection limits varied from 0.01 to 0.05  $\mu\text{g}/\text{m}^3$  for anions and from 0.02 to 0.07  $\mu\text{g}/\text{m}^3$  for cations. Blank values were used for calibration.  $\delta^{34}\text{S}$  was analyzed using an elemental analyzer (Flash 2000; Thermo Scientific) and an isotopic ratio mass spectrometer (Delta V Plus; Finnigan) in the State Key Laboratory of Organic Geochemistry in the Guangzhou Institute of Geochemistry. The  $\delta^{34}\text{S}$  values (‰) were corrected by multi-point correction ( $r^2 = 0.999$ ) based on three international standards (IAEA SO-6, IAEA SO-5, and NBS-127) and reported in the standard delta notation relative to the Vienna Canyon Diablo Troilite standard. The measured  $\delta^{34}\text{S}$  value of standards IAEA SO-6, IAEA SO-5, and NBS-127 was  $-33.9 \pm 0.18\text{‰}$  ( $n = 8$ ),  $0.23 \pm 0.15\text{‰}$  ( $n = 16$ ), and  $20.63 \pm 0.23\text{‰}$  ( $n = 8$ ) with an accuracy within  $\pm 0.33\text{‰}$  to the recommended values from the IAEA. The standard deviation of the isotopic measurements for samples was within  $\pm 0.35\text{‰}$ .

## 2.4. Bayesian mixing model

Dominant source apportionment of  $\text{SO}_2$  in the atmosphere was conducted using a Bayesian mixing model. In principle, the  $\delta^{34}\text{S}$ - $\text{SO}_2$  values in the atmosphere should range between the original values emitted from sources and the values reached under equilibrium fractionation conditions (Sinha et al., 2008). To apportion sources  $\text{SO}_2$  in the atmosphere, the  $\delta^{34}\text{S}$ - $\text{SO}_2$  values emitted from three main kinds of sources were calculated statistically as means and standard deviations.

Considering the significant overlap of the  $\delta^{34}\text{S}$  values between biogenic sulfur and coal combustion (Liu et al., 1996; Maruyama et al., 2000; Norman et al., 1999; Shang et al., 2016; Xue et al., 2020; Yetang et al., 1993; Zhang et al., 1995; Zhao et al., 2018; Zheng et al., 2018), there may be a large uncertainty in identifying the contributions of these two sources. Based on global sulfur budgets, biogenic sulfur emissions from terrestrial surfaces accounts for approximately 1% of atmospheric sulfur (Lei et al., 1997). Therefore, only two sources (coal combustion and oil combustion) were considered and corrected by the possible fractionation effect to be used in the present study (Table S5 and Fig. S3). Then, the correlated means and standard deviations of the two sources were incorporated into the Bayesian mixing model to carry out the source apportionment. The details of this approach are discussed in Text S3 and Text S4.

## 3. Results and discussion

### 3.1. Feasibility of using pas-QW to determine sulfate in air

The uptake profiles of  $\text{SO}_4^{2-}$  over time are shown in Fig. 1 for both YT and GZ, with raw data presented in Table S1. Linear uptakes of  $\text{SO}_4^{2-}$  for Pas-QW during the calibration exercise period were found by good linear correlations between the values of uptake volume and deployment time. Considering that no or little  $\text{SO}_2$  can be converted into  $\text{SO}_4^{2-}$  by heterogeneous oxidation of particle surfaces in the quartz wool disk, and aerosol  $\text{SO}_4^{2-}$  does not usually undergo the reverse reaction to form atmospheric  $\text{SO}_2$  under normal atmospheric conditions, thus most of the accumulated  $\text{SO}_4^{2-}$  in the quartz wool disk was from aerosol  $\text{SO}_4^{2-}$  during the sampling period. The average sampling rates of GZ and YT were 2.0 and 2.6  $\text{m}^3/\text{day}$ , respectively. Considering the principle of active sampling and passive sampling is not the same, all the samples of the two cities are put together. The  $\text{SO}_4^{2-}$  still exhibited near-linear uptake profiles and the average measured sampling rate of 2.3  $\text{m}^3/\text{day}$  (Fig. S4). The rate was slightly higher than those for particle-associated semi-volatile organic compounds, such as polyaromatic hydrocarbons (0.2–0.9  $\text{m}^3/\text{day}$ ) (Bohlin et al., 2014; Klanova et al., 2008), polychlorinated dioxins/furans (1.4–2.0  $\text{m}^3/\text{day}$ ) (Heo and Lee, 2014; Mari et al., 2008), and monosaccharides (1.1–1.5  $\text{m}^3/\text{day}$ ) (Jiang et al., 2018), and comparable to the recently reported sampling rates of trace metals (including titanium, iron, manganese, and aluminum) based on Pas-DD (1–3  $\text{m}^3/\text{day}$ ) (Gaga et al., 2019). In order to reflect the sampling rate as much as possible, two sampling calibrations were carried out in different seasons in North and South of China. The sampling time of YT is the northern winter with relatively high concentration of sulfate in the atmosphere during the coal heating time, while the sampling time of GZ is the southern summer accompanied by high intensity precipitation and low sulfate concentration. Although the growth trend of sulfate collected in the two cities is slightly different, the overall trend is the same and the sampling rate differed only slightly

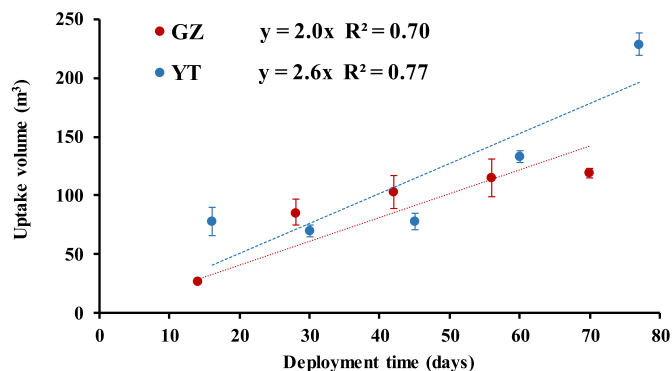


Fig. 1. Equivalent air volumes for Pas-QW for atmospheric sulfate based on measurements from conventional TSP samples at the in Yantai and Guangzhou field sites.

(Text S1). These findings indicated that the Pas-QW offered a feasible tool for monitoring studies, and the sampling rate was stable and not greatly affected by atmospheric sulfate concentration.

Sampling rates are not only influenced by the physicochemical properties of the target compounds, but may also be affected by atmospheric conditions, such as wind speed, temperature, humidity, and aerosol concentrations. It was found that the sampling rate was a function of wind speed, but the sampling rate was not significantly influenced by the wind speed when wind speeds is lower than 5 m/s (Herkert et al., 2018; Klanova et al., 2008). Information on correlations with other daily basic environmental and meteorological parameters in this study is given in Table S2. The wind speed was mostly lower than 3.4 m/s during the calibration study, which could be regarded as relatively low wind speed. Besides, sampling rate was not significantly correlated with daily basic environmental and meteorological parameters. This indicated that the effects of changes in meteorological parameters may be weakened during long-term sampling, and would not greatly affect the time-weighted average concentrations of  $\text{SO}_4^{2-}$  in a region.

To further verify the feasibility of using Pas-QW to collect atmospheric  $\text{SO}_4^{2-}$ , samples from five sites (BJ, SH, GZ, CD, and XM) were collected in March–June of 2017 and compared with previous studies conducted in the same regions and in the same year (Sun et al., 2019; Tian et al., 2019; Wang et al., 2019; Wu et al., 2019). The mass size distributions of sulfate is mainly in the accumulation mode, and the concentrations of sulfate in  $\text{PM}_{2.5}$  is about 60% of that in TSP (Fang et al., 2013; Lijiang, 2003; Wang et al., 2003). This study using quartz wool disks to collect target compounds from both of fine PM and coarse PM were still comparable to most of the previous studies conducted on  $\text{PM}_{2.5}$  samples, which have been corrected to the concentrations in

TSP (Sun et al., 2019; Tian et al., 2019; Wang et al., 2019; Wu et al., 2019). The results are shown in Fig. S5, and the comparison between the literature values and the measured values in this study is expressed as a ratio. Two values at the same site are in the same order of magnitude, and the variability of each site was within a factor of 2 (i.e., ratio between 0.5 and 2), consistent with the variability reported for passive air samplers in ambient air (Bohlin et al., 2014; Heo and Lee, 2014; Jiang et al., 2018; Mari et al., 2008). These indicated that the detected concentrations of  $\text{SO}_4^{2-}$  based on the derived average sampling rate in this study were comparable to the concentrations reported in the literature. The Pas-QW provides a direct and low-cost measurement of atmospheric sulfate across the regional scale.

### 3.2. Spatial distribution of sulfate and their isotopes and possible mechanisms

Spatial information on  $\text{SO}_4^{2-}$  air contents in Asia is provided in Fig. 2 and Table S3. During the sampling period, the temperature, relative humidity, and wind speed were within the range 9–34 °C ( $19.6 \pm 6.8$  °C), 36–81% ( $61.2 \pm 14.6\%$ ), and 1–4 m/s ( $2.4 \pm 0.9$  m/s), respectively. The meteorological parameters of these sampling sites were comparable to the range of the calibration exercise time, except for a few sites. Among the 29 sampling sites, the sampling sites of Pakistan, the ICP, and China had a range of 14.9–36.7  $\mu\text{g}/\text{d}$  ( $25.8 \pm 10.9$   $\mu\text{g}/\text{d}$ ), 9.1–44.6  $\mu\text{g}/\text{d}$  ( $19.8 \pm 12.9$   $\mu\text{g}/\text{d}$ ), and 11.6–79.4  $\mu\text{g}/\text{d}$  ( $48.8 \pm 20.3$   $\mu\text{g}/\text{d}$ ), respectively. The detected contents of background sites, rural sites, and urban sites had ranges of 12.9–28.6  $\mu\text{g}/\text{d}$  ( $20.8 \pm 7.8$   $\mu\text{g}/\text{d}$ ), 9.9–59.2  $\mu\text{g}/\text{d}$  ( $25.0 \pm 19.5$   $\mu\text{g}/\text{d}$ ), and 9.1–79.4  $\mu\text{g}/\text{d}$  ( $47.0 \pm 21.1$   $\mu\text{g}/\text{d}$ ), respectively. The lowest  $\text{SO}_4^{2-}$  content in both rural and urban sites

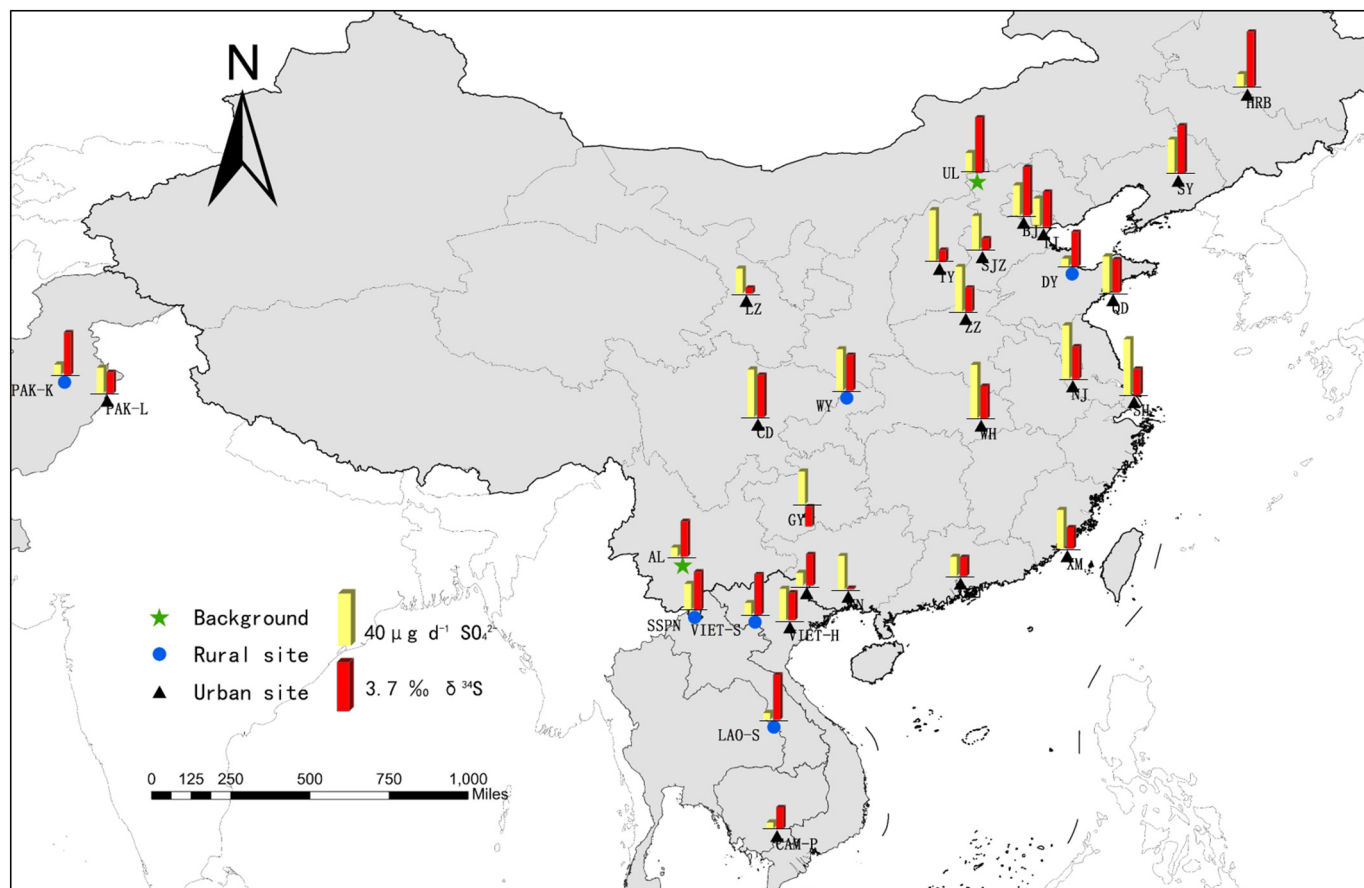


**Fig. 2.** Spatial distribution of sulfate air contents and  $\delta^{34}\text{S}$  in 29 sites of Asia. The contents of sulfate and  $\delta^{34}\text{S}$  values are indicated by yellow and red bar, respectively. The upward red bar represents positive  $\delta^{34}\text{S}$  value, and the downward red bar represents negative  $\delta^{34}\text{S}$  value.

were in the ICP. The highest  $\text{SO}_4^{2-}$  content was in Shanghai, located in the Yangtze River Delta in China. As a major commercial and financial center in mainland China, the annual total energy consumption in Shanghai increased from 31.91 to 118.59 million tons of coal equivalent in 1990 and 2017, respectively (Peng et al., 2019; Shanghai Municipal Statistics Bureau, 2017).

The average  $\delta^{34}\text{S}$  values of the three regions, as shown in Fig. 2 and Table S3, differed only slightly. The range of  $\delta^{34}\text{S}$  values observed in Pakistan ( $4.3 \pm 1.4\%$ ) and the ICP ( $4.5 \pm 1.2\%$ ) were relatively small, while a large range of  $\delta^{34}\text{S}$  values was observed in China ( $3.9 \pm 2.5\%$ ). Urban sites in southern China generally had lower isotope values than those in northern China. The highest isotope value was in Harbin (7.5%), located in northeastern China, with a high latitude and cold winters. Coal-fired heating and industrial emissions are the main source of atmospheric particulates in this city (Hong et al., 2019). Guiyang, located in southeastern China, had the lowest isotope value ( $-2.7\%$ ); the local coal in this area has been found to have a negative  $\delta^{34}\text{S}$  value (Maruyama et al., 2000; Mukai et al., 2001; Yetang et al., 1993).

There were large differences in atmospheric conditions and meteorological parameters between different sampling sites, which may have contributed to the regional distribution of  $\delta^{34}\text{S}$  values. Information on the correlations between  $\delta^{34}\text{S}\text{-SO}_4^{2-}$  and daily basic environmental parameters is shown in Table S4. There was a positive correlation between latitude and  $\delta^{34}\text{S}$  values ( $r = 0.41, p < 0.05$ ), suggesting that variations in conventional factors caused by latitude, such as wind speed, temperature, RH, and aerosol concentration, may result in variations in sulfur isotope fractionation factors. The regional distribution of  $\delta^{34}\text{S}\text{-SO}_4^{2-}$  may have been influenced by only factor or a combination of multiple factors. However, only a negative correlation was observed between RH and  $\delta^{34}\text{S}\text{-SO}_4^{2-}$  in aerosol ( $r = -0.40, p < 0.05$ ), and other factors were weakly correlated and not significant. High RH in atmosphere was favorable for  $\text{SO}_2$  dissolution and further oxidation by oxidants such as  $\text{H}_2\text{O}_2$ , ozone, oxygen gas, and nitrogen dioxide in atmosphere (Hung and Hoffmann, 2015), and ozone is strongly dependent on pH for the oxidation of  $\text{SO}_2$  (Sinha et al., 2008). Changes in RH can therefore affect the contribution of heterogeneous oxidation. However, the two study sites that had the same RH value (Lanzhou and Harbin) had completely different sulfur isotope compositions, and the two sites with the same sulfur isotope compositions (Wuhan and Nanjing), had different RH values. Thus, there are other important mechanisms leading to the regional distribution of  $\delta^{34}\text{S}$  in atmospheric  $\text{SO}_4^{2-}$ . Temperature is usually one of the most important meteorological boundary conditions, which may affect the observed seasonality in sulfur isotope compositions of aerosol  $\text{SO}_4^{2-}$  (Cheng et al., 2016; Han et al., 2016). Caron et al. (Caron et al., 1986) revealed that during the oxidation of  $\text{SO}_2$  into  $\text{SO}_4^{2-}$ , the  $\delta^{34}\text{S}\text{-SO}_4^{2-}$  value increased by 0.08–0.15‰ with a 1 °C decrease in temperature. However, the correlation between mean ambient temperature and  $\delta^{34}\text{S}\text{-SO}_4^{2-}$  observed in this study was weak and not significant ( $r = -0.18, p > 0.05$ ). This indicates that the influence of temperature changes may be weakened during the long-term sampling, and provides only a very small contribution to the regional variation in the sulfur isotope compositions. Although the influence of meteorological boundary conditions cannot be ruled out, they could not explain the regional distribution of  $\delta^{34}\text{S}$  values in atmospheric  $\text{SO}_4^{2-}$ .

### 3.3. Estimation of atmospheric sulfur sources from $\delta^{34}\text{S}$

$\text{SO}_4^{2-}$  in aerosols is derived from both primary (e.g., sea salt, dust, fly ash) and secondary (e.g., oxidation of  $\text{SO}_2$  and  $\text{H}_2\text{S}$ )  $\text{SO}_4^{2-}$  (Mukai et al., 2001; Norman et al., 2006), all characterized by their own distinct isotopic compositions. If sea salt is included in aerosols, it causes a positive bias to the  $\delta^{34}\text{S}$  value because of its heavy isotope composition (around 20.1‰) (Tostevin et al., 2014). Sea salt  $\text{SO}_4^{2-}$  is usually estimated from the sodium concentration. If all observed sodium is estimated to be from sea salt, its maximum increase to the  $\delta^{34}\text{S}$  value of samples could be calculated at 2.7‰ in these regions. However, because the  $\text{SO}_4^{2-}$

concentration was extremely high compared with the expected sea salt concentration, the estimated maximum contribution was, in most cases, under 0.6‰, even in seaside cities like Shanghai, Qingdao, Tianjin, and Xiamen. Since it was difficult to identify sea salt sodium from sodium from other sources (e.g., coal combustion and soil), sea salt correction was not performed, except on the samples from CAM-P and LAO-S where the contribution of sodium from sea salt may have been greater (Text S5 and Fig. S6). The contribution of sea salt concentration to  $\text{SO}_4^{2-}$  was 7.9% at CAM-P and 13.4% at LAO-S, and the sulfur isotope composition after sea salt correction was 1.3‰ for CAM-P and 3.4‰ for LAO-S.

The contribution from coal combustion to the atmospheric sulfur pool is generally significant, especially in China (Han et al., 2016; Mukai et al., 2001). Coals from different regions in China have different sulfur isotopic compositions, which may be the main factor leading to the regional distribution of  $\delta^{34}\text{S}\text{-SO}_4^{2-}$ . Although imported coal occupies a share of the Chinese coal market, its sulfur content is lower and it is burned in far smaller quantities compared to domestic coal. In 2017 (Bureau SS, n.d.; Xiao et al., 2018), coal imports accounted for less than 8% of domestic coal production (Xiao et al., 2018); therefore, only the sulfur isotope compositions of coal ( $\delta^{34}\text{S}_{\text{coal}}$ ) from near the sample sites was considered in this study. Fig. 3 shows the  $\delta^{34}\text{S}$  value of coals used near the sampling sites, oil and biogenic sulfur (Liu et al., 1996; Maruyama et al., 2000; Norman et al., 1999; Yetang et al., 1993; Zhang et al., 1995). The mean sulfur isotope composition of coal in southern China was generally lower than that in northern China, especially in Guiyang, where the lowest sulfur isotope value of coal ( $-12.0\text{--}-2.5\%$ ) was reported (Maruyama et al., 2000; Mukai et al., 2001; Xiao et al., 2015; Yetang et al., 1993). The sulfur content in oil from China was reported to vary from 0.1% to 0.6%, with an average  $\delta^{34}\text{S}$  value of  $11.6 \pm 6.7\%$  (Maruyama et al., 2000; Zhang et al., 2002). Terrestrial biogenic sulfur from vegetation, soil and wetland is a natural source of airborne sulfur, and has a low  $\delta^{34}\text{S}$  value of  $-10\%$  to  $-2\%$  (Mast et al., 2001). In this study, the range of  $\delta^{34}\text{S}\text{-SO}_4^{2-}$  in North China was 0.8–7.5‰, with the tendency corresponding well to the values of source coals (6.6‰) (Maruyama et al., 2000; Yetang et al., 1993). Sulfur isotopic composition varied greatly in southern coal due to regional differences, for example, the  $\delta^{34}\text{S}_{\text{coal}}$  ranges in the Pearl River Delta, Southeast China, and Southwest China were 3.1–6.7‰ (Liu et al., 1996; Xiao et al., 2015; Zhang et al., 1995; Zhang et al., 2010),  $-0.7\text{--}10.2\%$  (Chameides and Stelson, 1992; Zhang et al., 1995; Zhang et al., 2010), and  $-1.7\text{--}5.4\%$  (Yetang et al., 1993; Zhang et al., 2002; Zhang et al., 2010), respectively. The ranges of  $\delta^{34}\text{S}\text{-SO}_4^{2-}$  in the Pearl River Delta, Southeast China, and Southwest China was 3.5–4.4‰, 0.2–2.9‰, and 4.8–5.7‰, respectively, which were close to the  $\delta^{34}\text{S}_{\text{coal}}$  values at the sites. Therefore, coal combustion may be a significant, if not the most important contributor, to the atmospheric  $\text{SO}_4^{2-}$  pool.

Considering there existed a negative deviation of sulfur isotopic composition during combustion and flue gas desulfurization (FGD) (Derda et al., 2007; Yearbook, 2015; Zhao et al., 2018), the corrected  $\delta^{34}\text{S}\text{-SO}_2$  value after the sulfur isotopic fractionation effect was shown in Fig. 3. The results showed that the  $\delta^{34}\text{S}\text{-SO}_4^{2-}$  in this study was between the values of coal and oil combustion, indicating that atmospheric  $\text{SO}_4^{2-}$  was controlled by the two sources. Terrestrial biogenic sulfur were identified as an important source of airborne sulfur in the remote and rural areas, especially in environments with relatively high temperature and humidity, which leads to a significant increase in microbial activity in wetlands and soils (Lei et al., 1997; Zelong et al., 2020). However, only 1% of atmospheric sulfur (Lei et al., 1997), indicated that the contribution of terrestrial biogenic sulfur to atmospheric  $\text{SO}_4^{2-}$  pool in the areas with intensive human activities is negligible.

The sulfur isotope compositions of atmospheric  $\text{SO}_4^{2-}$  in Pakistan and the ICP are shown in Fig. S7. The average  $\delta^{34}\text{S}$  values of Pakistan and the ICP after sea salt correction range from 2.9 to 5.7‰ ( $4.3 \pm 1.4\%$ ), and from 1.2 to 5.5‰ ( $3.6 \pm 1.2\%$ ), respectively. Since  $\delta^{34}\text{S}$

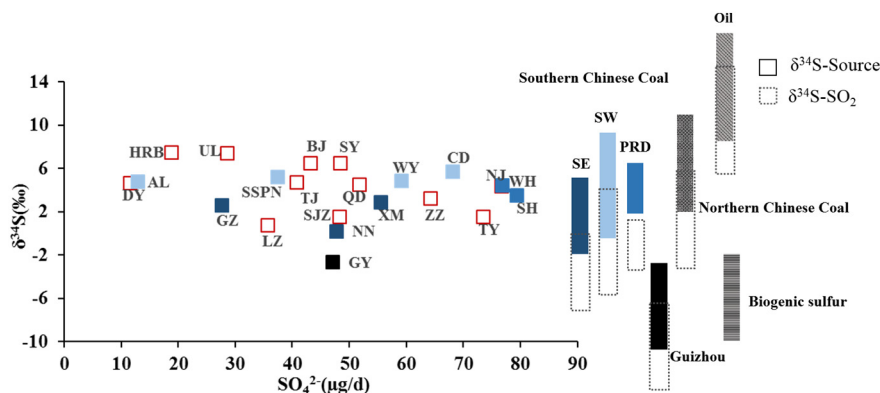


**Fig. 3.**  $\delta^{34}\text{S}$  values and atmospheric sulfate concentration in China compared to a ternary mixing model. The mean  $\delta^{34}\text{S}$  value (+6.6‰) of coal in North China is used. The range of  $\delta^{34}\text{S}_{\text{coal}}$  value in Southeast China is -1.7–5.4‰. The range of  $\delta^{34}\text{S}_{\text{coal}}$  value in Southwest China is -0.7–10.2‰ except Guiyang. The range of  $\delta^{34}\text{S}_{\text{coal}}$  value in Guiyang is -12.0–-2.5‰. The range of  $\delta^{34}\text{S}_{\text{coal}}$  value in PRD is 3.1–6.7‰. The mean  $\delta^{34}\text{S}$  value of oil (+11.6‰) and biogenic sulfur (-6.0‰) is used. The mean  $\delta^{34}\text{S}\text{-SO}_2$  value of coal combustion (-1.1 ± 5.2‰) and oil combustion (10.4 ± 6.7‰) is used. The dotted line represents the range of  $\delta^{34}\text{S}\text{-SO}_2$ , and the solid line represents the range of  $\delta^{34}\text{S}\text{-Source}$ .

values of Pakistan and the ICP were in a relatively narrow range, it is speculated that there were relatively stable sulfur sources during the sampling period. Considering their average  $\delta^{34}\text{S}$  values were close to those in China, the source of atmospheric  $\text{SO}_4^{2-}$  is likely to be approximate to China. However, there are no data on the sulfur source value of coal and oil in these two regions, further analysis and verification are required.

### 3.4. Source apportionment of $\text{SO}_2$ using a Bayesian model

Incorporating the isotopic fractionation of the equilibrium/Leighton reaction into the Bayesian model, the  $\delta^{34}\text{S}\text{-SO}_4^{2-}$  and  $\delta^{34}\text{S}\text{-SO}_2$  in the atmosphere can be linked (Han et al., 2016; Mukai et al., 2001; Norman et al., 2006). In this study, coal combustion (-1.1 ± 5.2‰) and oil combustion (10.4 ± 6.7‰) were considered to be the dominant artificial contributors of  $\text{SO}_2$  (Table S5). The contributions of coal combustion and oil combustion were within the ranges 45.4–96.8% (80.4 ± 13.1%) and 3.2–54.6% (19.6 ± 13.1%), respectively. The results showed that

coal combustion was the major source of  $\text{SO}_2$  in Asia, with the two sources differing greatly among regions. The current source apportionment methods of  $\text{SO}_2$  are based on air quality models and emission inventories, such as the Comprehensive Air Quality Model (CAMx) (Shimadera et al., 2015), Community Multiscale Air Quality (CMAQ) (Chen et al., 2020; Shimadera et al., 2015), and Multi-resolution Emission Inventory for China (MEIC) (Chen et al., 2019; He, 2012). However, these methods are usually accompanied by some level of uncertainty, resulting in source contributions that can differ in magnitude (Chen et al., 2019; Li et al., 2017a). Combining the sulfur isotope compositions analysis with a Bayesian model can provide effective constraint parameters for accurately creating  $\text{SO}_2$  emission inventories.

This finding differed from previous  $\text{SO}_2$  emission inventories (Fig. 4), which revealed the dominant role of coal combustion in China (Fig. S8) (Li et al., 2017a; Liu et al., 2015). Although previous studies have shown that coal combustion, especially in power plants, is the most important source of  $\text{SO}_2$  in China (Jia and Wang, 2017; Liu et al., 2015; Shang et al., 2016; Zheng et al., 2018), the widespread use of pollution control

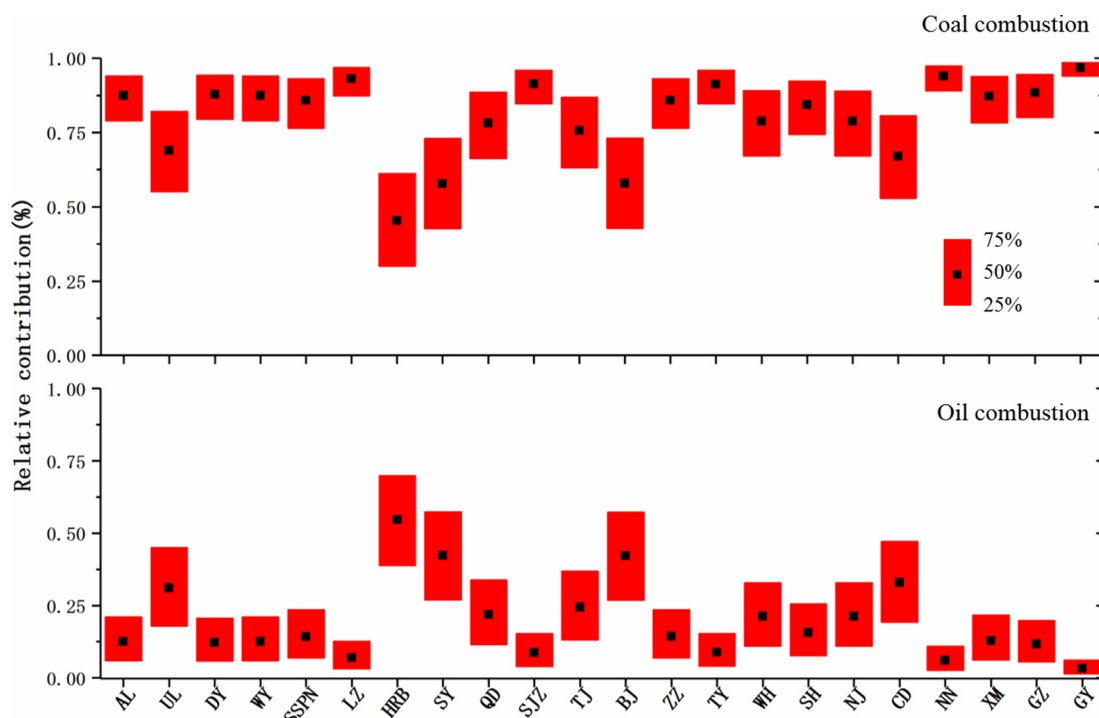


**Fig. 4.** Artificial sources contributions of  $\text{SO}_2$  in 22 sites of China obtained by Bayesian model.

devices on these plants has greatly reduced SO<sub>2</sub> emissions under the “Twelfth Five-Year Plan for National Environment Protection” in China. 99% of all power plants in China were installed with SO<sub>2</sub> removal systems by the end of 2015 (Shang et al., 2016). SO<sub>2</sub> emissions decreased from 104,000 tons in 2012 to 14,000 tons in 2017, an average decrease of 86.7%, with most of the decrease attributed to the reduction in emissions from power plants (Dai et al., 2019; Jia and Wang, 2017). Another major improvement is that China has implemented an ultra-low emissions standards policy since 2014, and has renovated coal-fired power generating units to limit the emission of various pollutants (Tang et al., 2019). According to the “Development Report on Desulfurization and Denitration Industry in 2017”, 71% of coal-fired power units have completed ultra-low emissions retrofits in China, and SO<sub>2</sub> emissions from power plants fully meet the most stringent international environmental standards (Tang et al., 2019; Zhao et al., 2018). By contrast, the explosive growth in car ownership in recent years has led to vehicle exhaust emissions becoming an important source of SO<sub>2</sub> pollution. According to automotive industry surveys, the average annual growth rate of car ownership in China reached a high of 14% from 2009 (Yearbook, 2015). Although the contribution of coal combustion to SO<sub>2</sub> pollution in this study was higher than vehicle exhaust emissions, it was much lower than reported in previous SO<sub>2</sub> emission inventories (Li et al., 2017a).

Industrial emissions of SO<sub>2</sub> mainly arise from coal-fired combustion (e.g., power plants, boiler combustion, etc.) (Dai et al., 2019; Jia and Wang, 2017; Tang et al., 2019; Zhao et al., 2018). Fig. 5 shows a comparison of the contribution of coal combustion obtained from the Bayesian model with the proportion of SO<sub>2</sub> emissions from industrial sources obtained from emission inventories in China (Jia and Wang, 2017). Most sites in China were more influenced by coal combustion, and the proportions of SO<sub>2</sub> emissions from industrial sources in emission inventories were comparable with the contributions from coal combustion obtained using the Bayesian model in some regions. This indicates that SO<sub>2</sub> emissions from heavy industries are still one of the most important sources of SO<sub>2</sub> emissions in China. However, in cities like Beijing (BJ) and Harbin (HRB), the contribution of coal combustion obtained using the Bayesian model is lower than that from other regions. The HRB sampling site was located in the Harbin Institute of Technology, which is in the business district and surrounded by busy traffic. Local transportation may lead to higher contributions of oil sources to SO<sub>2</sub>. The BJ sampling site was located in Peking University, and subject to local heavy traffic from tertiary industries such as tourism. (Jia and Wang, 2017). This suggests that changes in the energy structure caused by industrial transfer and upgrading in China lead to changing SO<sub>2</sub> emissions and source contributions in different regions. In addition, for rural and background sites, household coal combustion is an important source of sulfur emissions. Considering the combustion of civil coal does not perform flue gas desulfurization (FGD), the parameter of the Bayesian model was adjusted and the fractionation of FGD process was not included in these two regions. The results showed that coal combustion is still the dominant contributors to SO<sub>2</sub> in rural and background sites, and the

contributions obtained from the Bayesian model were comparable to average value of the region from SO<sub>2</sub> emission inventories (Jia and Wang, 2017). And a certain proportion of oil combustion indicated that the contribution of vehicle exhaust emissions to SO<sub>2</sub> cannot be ignored even in the remote areas.

#### 4. Conclusions

Our study developed a new method for measuring atmospheric  $\delta^{34}\text{S}\text{-SO}_4^{2-}$  over large regions, and carried out a field study at 29 sites in three parts of Asia, then combined real isotopic data and the Bayesian model to quantitatively apportion the respective contribution of major artificial sources. Important findings of this study include 1) sulfate exhibited near-linear uptake profiles with the mass collected on the samplers proportional to the deployment time, and the average sampling rate of sulfate collected by Pas-QW was  $2.3 \pm 0.3 \text{ m}^3/\text{d}$ ; 2) results of simultaneous sampling and analysis showed the spatial distribution of sulfate contents were largely attributed to the development of regional economy, and the regional distribution of sulfur isotope compositions was more affected by coal combustion; 3) the two artificial sources (coal and oil combustion) differed greatly between regions, and the contribution of fuel oil should be seriously considered in plans to reduce SO<sub>2</sub> emissions. It should be noted that there was large uncertainty in the evaluation of coal and oil combustion source contributions obtained from the Bayesian model, which was partly ascribed to the lack of updating  $\delta^{34}\text{S}$  values from different sources. It was recommended to increase the adequate quantification of sulfur isotopes compositions from major SO<sub>2</sub> sources by undertaking actual measurements. In addition, the isotopic fractionation from the conversion of SO<sub>2</sub> to SO<sub>4</sub><sup>2-</sup> was simplified in this study, and it was impossible to incorporate all possible equilibrium and kinetic fractionation scenarios. However, this study developed a novel method to apportion SO<sub>2</sub> sources that will provide effective constraint parameters for accurate formulation of an SO<sub>2</sub> source emission inventory.

#### CRedit authorship contribution statement

**Xiao Wang:** Writing – original draft, Visualization, Data curation, Methodology, Software, Investigation, Writing – review & editing. **Jun Li:** Conceptualization, Methodology, Supervision, Validation, Writing – review & editing, Project administration, Funding acquisition. **Rong Sun:** Investigation, Methodology, Visualization. **Hongxing Jiang:** Investigation, Methodology, Visualization. **Zheng Zong:** Investigation, Methodology, Visualization. **Chongguo Tian:** Conceptualization, Methodology, Supervision, Validation, Data curation, Methodology, Writing – review & editing. **Luhua Xie:** Investigation, Methodology. **Qilu Li:** Conceptualization, Methodology, Supervision, Validation, Data curation, Methodology, Writing – review & editing. **Wanglu Jia:** Investigation, Methodology. **Ping'an Peng:** Methodology, Supervision, Validation. **Gan Zhang:** Methodology, Supervision, Validation.

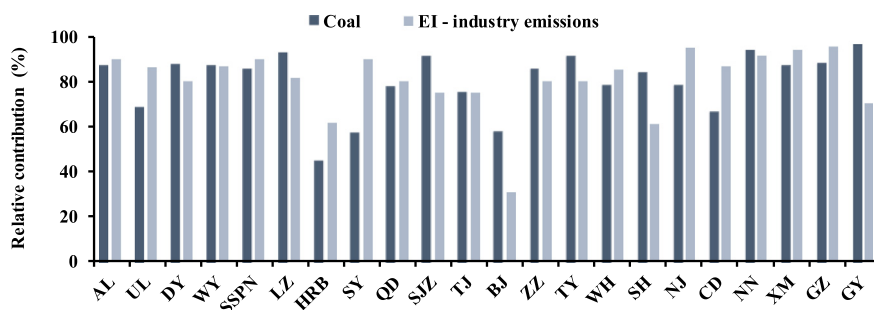


Fig. 5. A comparison of the contribution of coal combustion obtained from the Bayesian model and the proportion of SO<sub>2</sub> emissions of industrial sources in emission inventories.

## Declaration of competing interest

The authors declare that they have no known competing financial interests or personal relationships that could have appeared to influence the work reported in this paper.

## Acknowledgments

This study was supported by the Natural Science Foundation of China (NSFC; Nos. 41977177), State Key Laboratory of Organic Geochemistry, GIGCAS (Grant No. SKLOG 2020-05), Guangzhou Science and Technology Project (No. 201804010344), Guangdong Foundation for Program of Science and Technology Research (Grant No. 2017B030314057, 2019B121205006 and 2020B1212060053), and Guangdong Provincial Science and Technology projects: Guangdong-Hong Kong-Macao Greater Bay Area Urban agglomeration ecosystem Observation and Research Station (2018B030324002).

## Appendix A. Supplementary data

Supplementary data to this article can be found online at <https://doi.org/10.1016/j.scitotenv.2021.146107>.

## References

- Abbatt, J.P.D., Benz, S., Cziczo, D.J., Kanji, Z.A., Lohmann, U., Mohler, O., 2006. Solid ammonium sulfate aerosols as ice nuclei: a pathway for cirrus cloud formation. *Science* 313, 1770–1773.
- Amrani, A., Said-Ahmad, W., Shaked, Y., Kiene, R.P., 2013. Sulfur isotope homogeneity of oceanic DMSP and DMS. *Proc. Natl. Acad. Sci. U. S. A.* 110, 18413–18418.
- Bohlin, P., Audy, O., Skrdlikova, L., Kukucka, P., Vojta, S., Pribylova, P., et al., 2014. Evaluation and guidelines for using polyurethane foam (PUF) passive air samplers in double-dome chambers to assess semi-volatile organic compounds (SVOCs) in non-industrial indoor environments. *Environ. Sci. Process. Impact* 16, 2617–2626.
- Bureau SS. National database [EB/OL] <http://www.stats.gov.cn/tjsj/>.
- Calhoun, J.A., Bates, T.S., Charlson, R.J., 1991. Sulfur isotope measurement of submicrometer sulfate aerosol-particles over the pacific-ocean. *Geophys. Res. Lett.* 18, 1877–1880.
- Caron, F., Tessier, A., Kramer, J.R., Schwarcz, H.P., Rees, C.E., 1986. Sulfur and oxygen isotopes of sulfate in precipitation and lakewater, Quebec, Canada. *Appl. Geochem.* 1, 601–606.
- Chameides, W.L., Stelson, A.W., 1992. Aqueous-phase chemical processes in deliquescent sea-salt aerosols—a mechanism that couples the atmospheric cycles of sand sea salt. *J. Geophys. Res.-Atmos.* 97, 20565–20580.
- Charlson, R.J., Schwartz, S.E., Hales, J.M., Cess, R.D., Coakley, J.A., Hansen, J., et al., 1992. Climate forcing by anthropogenic aerosols. *Science* 255, 423–430.
- Chen, Y.Y., Ebenstein, A., Greenstone, M., Li, H.B., 2013. Evidence on the impact of sustained exposure to air pollution on life expectancy from China's Huai River policy. *Proc. Natl. Acad. Sci. U. S. A.* 110, 12936–12941.
- Chen, D., Liu, Z.Q., Ban, J.M., Chen, M., 2019. The 2015 and 2016 wintertime air pollution in China: SO<sub>2</sub> emission changes derived from a WRF-Chem/EnKF coupled data assimilation system. *Atmos. Chem. Phys.* 19, 8619–8650.
- Chen, D.S., Fu, X.Y., Guo, X.R., Lang, J.L., Zhou, Y., Li, Y., et al., 2020. The impact of ship emissions on nitrogen and sulfur deposition in China. *Sci. Total Environ.* 708, 11.
- Cheng, Y.F., Zheng, G.J., Wei, C., Mu, Q., Zheng, B., Wang, Z.B., et al., 2016. Reactive nitrogen chemistry in aerosol water as a source of sulfate during haze events in China. *Sci. Adv.* 2, 11.
- Dai, Q.L., Bi, X.H., Song, W.B., Li, T.K., Liu, B.S., Ding, J., et al., 2019. Residential coal combustion as a source of primary sulfate in Xi'an, China. *Atmos. Environ.* 196, 66–76.
- Demirel, G., Ozden, O., Dogeroglu, T., Gaga, E.O., 2014. Personal exposure of primary school children to BTEX, NO<sub>2</sub> and ozone in Eskisehir, Turkey: relationship with indoor/outdoor concentrations and risk assessment. *Sci. Total Environ.* 473, 537–548.
- Derda, M., Chmielewski, A.G., Licki, J., 2007. Sulphur isotope compositions of components of coal and S-isotope fractionation during its combustion and flue gas desulfurization. *Isot. Environ. Health Stud.* 43, 57–63.
- Eng, A., Harner, T., Pozo, K., 2014. A prototype passive air sampler for measuring dry deposition of polycyclic aromatic hydrocarbons. *Environ. Sci. Technol. Lett.* 1, 77–81.
- Fang, G.-C., Wu, Y.-S., Lin, S.M., Lin, C.-H., 2013. Study of ambient air particulates (particulate matter [PM]<sub>2.5</sub>, PM<sub>10</sub>, and Total suspended particulates [TSP]) ionic species concentrations in Asian countries during 1995–2009. *Environ. Forensic* 14, 121–132.
- Gaga, E.O., Harner, T., Dabek-Zlotorzynska, E., Celso, V., Evans, G., Jeong, C.H., et al., 2019. Polyurethane foam (PUF) disk samplers for measuring trace metals in ambient air. *Environ. Sci. Technol. Lett.* 6, 545–550.
- Han, X.K., Guo, Q.J., Liu, C.Q., Fu, P.Q., Strauss, H., Yang, J.X., et al., 2016. Using stable isotopes to trace sources and formation processes of sulfate aerosols from Beijing, China. *Sci. Rep.* 6, 14.
- He KB. Multi-resolution emission Inventory for China (MEIC): model framework and 1990–2010 anthropogenic emissions, in: Presented on the international Global Atmospheric Chemistry Conference, 17–21, September, Beijing, China, 2012.
- Heo, J., Lee, G., 2014. Field-measured uptake rates of PCDDs/fs and dl-PCBs using PUF-disk passive air samplers in Gyeonggi-do, South Korea. *Sci. Total Environ.* 491, 42–50.
- Herkert, N.J., Spak Scott, N., Smith, A., Schuster, J.K., Harner, T., Martinez, A., et al., 2018. Calibration and evaluation of PUF-PAS sampling rates across the global atmospheric passive sampling (GAPS) network. *Environ. Sci. Process. Impact* 20, 210–219.
- Hong, Y., Ma, Y.J., Sun, J.Y., Li, C.L., Zhang, Y.H., Li, X.L., et al., 2019. Water-soluble ion components of PM<sub>10</sub> during the winter-spring season in a typical polluted city in North-east China. *Environ. Sci. Pollut. Res.* 26, 7055–7070.
- Hung, H.M., Hoffmann, M.R., 2015. Oxidation of gas-phase SO<sub>2</sub> on the surfaces of acidic microdroplets: implications for sulfate and sulfate radical anion formation in the atmospheric liquid phase. *Environ. Sci. Technol.* 49, 13768–13776.
- Jia, F.P., Wang, G., 2017. Analysis of sulfur dioxide emission in China (in Chinese). *Ningbo Energy-saving* 16–25.
- Jiang, H.Y., Zhong, G.C., Wang, J.Q., Jiang, H.X., Tian, C.G., Li, J., et al., 2018. Using polyurethane foam-based passive air sampling technique to monitor monosaccharides at a regional scale. *Environ. Sci. Technol.* 52, 12546–12555.
- Klanova, J., Eupr, P., Kohoutek, J., Harner, T., 2008. Assessing the influence of meteorological parameters on the performance of polyurethane foam-based passive air samplers. *Environ. Sci. Technol.* 42, 550–555.
- Kunasek, S.A., Alexander, B., Steig, E.J., Sofen, E.D., Jackson, T.L., Thiemens, M.H., et al., 2010. Sulfate sources and oxidation chemistry over the past 230 years from sulfur and oxygen isotopes of sulfate in a West Antarctic ice core. *J. Geophys. Res.-Atmos.* 115, 13.
- Lei, H.-C., Tanner, P.A., Huang, M.-Y., Shen, Z.-L., Wu, Y.-X., 1997. The acidification process under the cloud in Southwest China: observation results and simulation. *Atmos. Environ.* 31, 851–861.
- Li, M., Zhang, Q., Kurokawa, J., Woo, J.H., He, K.B., Lu, Z.F., et al., 2017a. MIX: a mosaic Asian anthropogenic emission inventory under the international collaboration framework of the MICS-Asia and HTAP. *Atmos. Chem. Phys.* 17, 935–963.
- Li, W.J., Xu, L., Liu, X.H., Zhang, J.C., Lin, Y.T., Yao, X.H., et al., 2017b. Air pollution-aerosol interactions produce more bioavailable iron for ocean ecosystems. *Sci. Adv.* 3, 6.
- Lijiang, X., 2003. Environmental Chemistry [M]. 2003. China Environmental Science Press, Beijing.
- Liu, G.S., Hong, Y.T., Piao, H.C., et al., 1996. Study on sources of sulfur in atmospheric particulate matter with stable isotope method (in Chinese). *China. Environ. Sci.* 27–30.
- Liu, F., Zhang, Q., Tong, D., Zheng, B., Li, M., Huo, H., et al., 2015. High-resolution inventory of technologies, activities, and emissions of coal-fired power plants in China from 1990 to 2010. *Atmos. Chem. Phys.* 15, 13299–13317.
- Mari, M., Schuhmacher, M., Feliubadaló, J., Domingo, J.L., 2008. Air concentrations of PCDD/fs, PCBs and PCNs using active and passive air samplers. *Chemosphere* 70, 1637–1643.
- Maruyama, T., Ohizumi, T., Taneoka, Y., Minami, N., Fukuzaki, N., Mukai, H., et al., 2000. Sulfur isotope ratios of coals and oils used in China and Japan. *Nippon Kagaku Kaishi* 45–51.
- Mast, M.A., Turk, J.T., Ingersoll, G.P., Clow, D.W., Kester, C.L., 2001. Use of stable sulfur isotopes to identify sources of sulfate in Rocky Mountain snowpacks. *Atmos. Environ.* 35, 3303–3313.
- Matsumoto, K., Tanaka, H., Nagao, I., Ishizaka, Y., 1997. Contribution of particulate sulfate and organic carbon to cloud condensation nuclei in the marine atmosphere. *Geophys. Res. Lett.* 24, 655–658.
- Mukai, H., Tanaka, A., Fujii, T., Zeng, Y.Q., Hong, Y.T., Tang, J., et al., 2001. Regional characteristics of sulfur and lead isotope ratios in the atmosphere at several Chinese urban sites. *Environ. Sci. Technol.* 35, 1064–1071.
- Norman, A.L., Barrie, L.A., Toom-Sauntry, D., Sirois, A., Krouse, H.R., Li, S.M., et al., 1999. Sources of aerosol sulphate at alert: apportionment using stable isotopes. *J. Geophys. Res.-Atmos.* 104, 11619–11631.
- Norman, A.-L., Anlauf, K., Hayden, K., Thompson, B., Brook, J.R., Li, S.-M., et al., 2006. Aerosol sulphate and its oxidation on the Pacific NW coast: S and O isotopes in PM<sub>2.5</sub>. *Atmos. Environ.* 40, 2676–2689.
- Ohizumi, T., Take, N., Inomata, Y., Yagoh, H., Endo, T., Takahashi, M., et al., 2016. Long-term variation of the source of sulfate deposition in a leeward area of Asian continent in view of sulfur isotopic composition. *Atmos. Environ.* 140, 42–51.
- Peng, X., Liu, M., Zhang, Y., Meng, Z., Achal, V., Zhou, T., et al., 2019. The characteristics and local-regional contributions of atmospheric black carbon over urban and suburban locations in Shanghai, China. *Environ. Pollut.* 255, 113188.
- Pope, C.A., Dockery, D.W., 2006. Health effects of fine particulate air pollution: lines that connect. *J. Air Waste Manage. Assoc.* 56, 1368–1380.
- Shang, X.G., Si, C.H., Y., L., 2016. Industrial policy guiding and development trend of dust removal, Desulfurization and Denitration in the Thirteenth Five-Year Plan. *China Environ. Protect. Ind.* 10.
- Shanghai Municipal Statistics Bureau, 2017. Shanghai Statistical Yearbook. <http://tjj.sh.gov.cn/tjnj/20190117/0014-1001529.html>.
- Shimadera, H., Kojima, T., Kondo, A., Inoue, Y., 2015. Performance comparison of CMAQ and CAMx for one-year PM<sub>2.5</sub> simulation in Japan. *Int. J. Environ. Pollut.* 57, 146–161.
- Sinha, B., Hoppe, P., Huth, J., Foley, S.F., Andreae, M.O., 2008. Sulfur isotope analyses of individual aerosol particles in the urban aerosol at a central European site (Mainz, Germany). *Atmos. Chem. Phys.* 8, 7217–7238.
- Sun, W., Wang, D., Yao, L., Fu, H., Fu, Q., Wang, H., et al., 2019. Chemistry-triggered events of PM<sub>2.5</sub> explosive growth during late autumn and winter in Shanghai, China. *Environ. Pollut.* 254, 112864.
- Tang, L., Qu, J.B., Mi, Z.F., Bo, X., Chang, X.Y., Anadon, L.D., et al., 2019. Substantial emission reductions from Chinese power plants after the introduction of ultra-low emissions standards. *Nat. Energy* 4, 929–938.
- Tian, M., Liu, Y., Yang, F., Zhang, L., Peng, C., Chen, Y., et al., 2019. Increasing importance of nitrate formation for heavy aerosol pollution in two megacities in Sichuan Basin, Southwest China. *Environ. Pollut.* 250, 898–905.



- Tostevin, R., Turchyn, A.V., Farquhar, J., Johnston, D.T., Eldridge, D.L., Bishop, J.K.B., et al., 2014. Multiple sulfur isotope constraints on the modern sulfur cycle. *Earth Planet. Sci. Lett.* 396, 14–21.
- Wang, G., Wang, H., Yu, Y., Gao, S., Feng, J., Gao, S., et al., 2003. Chemical characterization of water-soluble components of PM10 and PM2.5 atmospheric aerosols in five locations of Nanjing, China. *Atmos. Environ.* 37, 2893–2902.
- Wang, Y., Zhang, H., Zhai, J., Wu, Y., Cong, L., Yan, G., et al., 2019. Seasonal variations and chemical characteristics of PM2.5 aerosol in the urban Green Belt of Beijing, China. *Pol. J. Environ. Stud.* 29, 361–370.
- Wu, X., Xu, L., Hong, Y., Chen, J., Qiu, Y., Hu, B., et al., 2019. The air pollution governed by subtropical high in a coastal city in Southeast China: formation processes and influencing mechanisms. *Sci. Total Environ.* 692, 1135–1145.
- Xiao, H.-Y., Li, N., Liu, C.-Q., 2015. Source identification of sulfur in uncultivated surface soils from four Chinese provinces. *Pedosphere* 25, 140–149.
- Xiao, X.J., Gao, H., Zhang, Y.S., 2018. Review of China's coal development in 2017 and outlook and suggestions for 2018 (in Chinese). *Energ. China* 40, 5–9.
- Xue, Y.F., Zhang, S.H., Nie, T., Cao, X.Z., Shi, A.J., 2020. Environmental effective assessment of control measures implemented by clean air action plan (2013–2017) in Beijing, China. *Atmosphere* 11, 12.
- Yearbook, C.S., 2015. Part XVI: Transport, Post, and Telecommunication Services. China Statistics Press, Beijing.
- Yetang, H., Hongbin, Z., Yongxuan, Z., 1993. Sulfur isotopic characteristics of coal in China and sulfur isotopic fractionation during coal-burning process. *Chin. J. Geochem.* 12, 51–59.
- Zelong, Y., Xiaokun, H., Lang, Y., Guo, Q., Li, S., 2020. The abatement of acid rain in Guizhou province, southwestern China: implication from sulfur and oxygen isotopes. *Environ. Pollut.* 267, 115444.
- Zhang, H.B., Chen, Y.W., Liu, D.P., 1995. Study on sulfur source of acid rain using sulfur isotopic trace (in Chinese). *Geochimica* 126–133.
- Zhang, H.B., et al., 2002. Sulfur isotopic composition of acid deposition in South China Regions and its environmental significance (in Chinese). *China Environ. Sci.* 70–74.
- Zhang, M., Wang, S., Ma, G., Zhou, H., Fu, J., 2010. Sulfur isotopic composition and source identification of atmospheric environment in central Zhejiang, China. *Sci. China Earth Sci.* 53, 1717–1725.
- Zhao X, Cheng X, Hou JX. Development Report on Desulfurization and Denitration Industry in 2017 (In Chinese). China Environmental Protection Industry 2018: 10–24.
- Zheng, B., Tong, D., Li, M., Liu, F., Hong, C.P., Geng, G.N., et al., 2018. Trends in China's anthropogenic emissions since 2010 as the consequence of clean air actions. *Atmos. Chem. Phys.* 18, 14095–14111.
- Zong, Z., Wang, X.P., Tian, C.G., Chen, Y.J., Fang, Y.T., Zhang, F., et al., 2017. First assessment of NO<sub>x</sub> sources at a regional background site in North China using isotopic analysis linked with modeling. *Environ. Sci. Technol.* 51, 5923–5931.